

# Narrow Band Pressure Computation for Eulerian Fluid Simulation

Aditya Prakash and Parag Chaudhuri

*Department of Computer Science and Engineering, Indian Institute of Technology Bombay, Mumbai, India*

**Keywords:** Eulerian Fluid Simulation, Narrow Band Pressure Solve, Fluid Animation.

**Abstract:** An Eulerian fluid simulation for incompressible fluids spends a lot of time in enforcing incompressibility by solving a large Poisson's equation. This involves solving a large system of equations using a solver like conjugate gradients. We introduce a way of accelerating this computation by dividing the grid domain of the fluid simulation into a narrow band of high resolution grid cells near fluid-solid boundaries and a coarser grid everywhere else. Judiciously reducing the number of high resolution grid cells significantly lowers the cost of the pressure projection step, while not sacrificing the simulation quality. The coarse grid values are upgraded to a finer grid before advecting the fluid surface so that enough degrees of freedom are available to resolve surface detail. We present and analyse two methods to perform this upgradation, namely, velocity interpolation and pressure field smoothing. We discuss the merits and demerits of each and quantify the errors introduced in the simulation as a function of size of the narrow band. Finally, since we are primarily interested in visualizing the fluid animation, we produce rendered fluid simulation output to also validate the visual quality of the simulations.

## 1 INTRODUCTION

Eulerian fluid simulation involves solving the Navier-Stokes equations on a fixed grid. An incompressible fluid solve on a regular rectilinear grid is a common example of this kind of simulation. Even in its simplest setting this a computationally intensive task, and a major proportion of this computation is spent in the pressure projection stage that enforces fluid incompressibility (Lentine et al., 2010; Prakash and Chaudhuri, 2015). This is done by solving a Poisson's equation using an iterative or direct solver.

A lot of earlier research has attempted to increase the speed of pressure projection on fixed grids. These methods are either not tailored for visual liquid simulation (Montijn et al., 2006), or use specific complicated grid structures (Ferstl et al., 2014), or treat the fluid free surface differently from rest of the fluid volume (Autodesk, ). Dimension reduction techniques (Treuille et al., 2006) and different basis functions (De Witt et al., 2012) have also been used for this purpose. The problem however, remains challenging for liquids simulation as the fluid volume topology changes rapidly and enforcing correct boundary conditions is difficult.

We specifically focus on visual fluid (liquid) animation and present a technique to accelerate the pres-

sure solve by creating a very coarse grid for the entire fluid simulation, except for a narrow band of fine grid cells around the boundary. This grid structure is statically determined and does not require runtime re-gridding. It perfectly enforces both Dirichlet and Neumann boundary conditions at the fluid free surface and fluid-solid boundary. We avoid the pitfalls of the previous methods while still managing to maintain enough degrees of freedom in the final velocity field of the fluid simulation so as to be able to generate adequate surface detail. Our specific contributions are as follows:

1. We present a simple, flexible method to reduce the size of the pressure projection problem by using a coarser grid and a narrow band fine grid. We show how to couple these together to enforce both free surface and fluid-solid boundary conditions.
2. We show how to upgrade values from the coarse grid back to a fine grid to get adequate degrees of freedom in the velocity field to represent surface detail using two techniques, namely, velocity interpolation and pressure field smoothing.
3. We rigorously compare the speedups obtained in computation while using the two upgradation strategies. We also quantify the errors introduced due to our methods, and the visual quality of the simulation thus produced, in both 2D and 3D.

These ideas substantially reduce the computational cost of the pressure solve without compromising on simulation quality. Our method is also easy to parallelize and works perfectly on multi-core architectures.

We start by looking at existing literature in the concerned area in Section 2. We briefly discuss the details of the Navier-Stokes equation and the Poisson's equation that requires most of the computational effort to solve during the simulation in Section 3. We follow this up with a detailed description of our narrow band pressure solve method and all the algorithms in Section 4. We compare the performance of our algorithms, the visual and timings results obtained and the errors involved in Section 5. We conclude in Section 6 with a brief summary and discussion about limitations of the current system and possible future directions.

## 2 BACKGROUND

Grid-based Eulerian simulation of incompressible fluids is commonly used for visual fluid animation in computer graphics and scientific visualization. Many authors have presented systems that present visually compelling results from fluid simulations on Eulerian grids (Stam, 1999; Foster and Fedkiw, 2001; Enright et al., 2002), however, the size of the grids that these techniques can use is limited by computational power available.

As a consequence of this, many authors have looked at adding details to these simulations by adding various kinds of noise, like Kolmogorov noise (Larmorlette and Foster, 2002; Rasmussen et al., 2003) or curl noise (Bridson et al., 2007). Some techniques (Schechter and Bridson, 2008) determine where to add the noise and couple it to the Navier-Stokes equations. However, these are not physically realistic techniques and do not produce convincing details in all situations.

Another approach is to improve the original simulation by the particular choice of the methods used to solve each stage depending on accuracy, stability and computational cost. E.g. semi-Lagrangian advection, proposed by Stam et al. (Stam, 1999) is unconditionally stable but has only first order accuracy, whereas Selle et al. (Selle et al., 2008) used a modified McCormack scheme to give second order accuracy to the advection step. Another way is to try and maintain certain invariants like energy (Mullen et al., 2009) during the simulation. These methods increase accuracy and fidelity of the simulation, but they involve more expensive computation and are still limited by

the grid resolution on which the simulation is performed. In order to increase grid resolution without too much computational cost, some authors have introduced adaptive grid techniques like AMR (Berger and Oliger, 1984) and octrees (Losasso et al., 2004), however, these complicated data structures are difficult to update during simulation and robust numerical solutions are difficult to design on such grids.

Lentine et al. (Lentine et al., 2010) present a method of using a multi-resolution grid to speedup the pressure projection step. They also require the velocity field to be interpolated from a lower resolution to a higher one. We show in this paper that velocity interpolation is a poorer speedup strategy as forcing the velocity field to be divergence free is harder post interpolation and leads to lower speedups than other methods.

Other authors have presented multigrid techniques for efficiently solving Poisson problems (McAdams et al., 2010; Chentanez and Müller, 2011; Jung et al., 2013). Though theoretically multigrid techniques are very efficient, they require precise discretization and complicated data-structures for correctly converging on regular grids (Ferstl et al., 2014). Our method is much easier to apply and is guaranteed to converge.

Ando et. al (Ando et al., 2015) describe the work that is closest to ours in spirit. They also describe a dimension reduction strategy for simplifying the pressure solve. Their work uses an up-sampling matrix to interpolate the pressure to a higher resolution grid during the pressure solve. They enforce Dirichlet boundary conditions by using a surface aware pressure basis to make the pressure zero at the free surface. Our method is closely related to this work in that we too present a dimension reduction strategy in that interpolates pressure to a higher resolution grid, after the linear pressure solve. In addition we compute pressure at higher resolution in a narrow band around the fluid-solid boundary. This gives a better solution in this boundary region. Our method is also easier to understand and implement.

Authors have also investigated hybrid Eulerian-Lagrangian methods to achieve speedup in fluid simulation computations. Chentanez et. al (Chentanez et al., 2014) couple a Eulerian solver, a shallow water solver and a Lagrangian SPH solver within a simulation. The material point method (MPM) combines a grid-based Eulerian simulation with marker particles to simulate a range of materials like snow (Stomakhin et al., 2013) and foams (Yue et al., 2015). Ferstl et. al (Ferstl et al., 2016) present a solution for accelerating FLIP advection in Eulerian grid-based fluid simulations by using FLIP particles only in a narrow band around the free surface of the fluid.

Some authors have also experimented with addition of high resolution detail to low-resolution simulations (Threy et al., 2010; Kim et al., 2013) but these are largely orthogonal to the techniques presented in this paper.

### 3 THE NAVIER-STOKES EQUATIONS

The Navier-Stokes for inviscid, incompressible fluids is given by the pair of equations given below. These equations govern the conservation of momentum and mass of the fluid.

$$\frac{\partial \mathbf{u}}{\partial t} + \mathbf{u} \cdot \nabla \mathbf{u} = -\frac{1}{\rho} \nabla p + \mathbf{f} \quad (1)$$

$$\nabla \cdot \mathbf{u} = 0, \quad (2)$$

where  $\rho$  is the density,  $\mathbf{u}$  the velocity,  $p$  the pressure, and  $\mathbf{f}$  the acceleration due to an external force, such as gravity. We solve these equations by operator splitting. For any given iteration,  $n$ , and corresponding fluid velocity,  $\mathbf{u}^n$ , first the advection step is solved and an intermediate velocity,  $\mathbf{u}^*$ , is computed.  $\Delta t$  is the timestep of the solver.

$$\frac{\mathbf{u}^* - \mathbf{u}^n}{\Delta t} + \mathbf{u}^n \cdot \nabla \mathbf{u}^n = \mathbf{f}. \quad (3)$$

The pressure is computed next by solving a Poisson system of the form

$$\nabla \cdot \frac{\Delta t}{\rho} \nabla p = \nabla \cdot \mathbf{u}^*. \quad (4)$$

Subsequently, the pressure forces are added to compute the velocity for the next iteration, i.e.,  $\mathbf{u}^{n+1}$ .

$$\frac{\mathbf{u}^{n+1} - \mathbf{u}^*}{\Delta t} = -\frac{1}{\rho} \nabla p. \quad (5)$$

The domain in which Equations 3, 4 and 5 are solved is tracked by a distance field  $\phi$ , where  $\phi < 0$  for regions that contain the fluid. The level-set is evolved with the fluid by solving

$$\frac{\partial \phi}{\partial t} = -\mathbf{u} \cdot \nabla \phi. \quad (6)$$

Solving the Poisson system (in Equation 4) is a substantial computational component of the entire fluid solve (Lentine et al., 2010; Prakash and Chaudhuri, 2015). Therefore, solving this on a coarse grid reduces computational complexity substantially. A coarse grid, however, cannot capture adequate fluid surface detail, thus making high resolution or finer grids essential.

We solve the Poisson system on a coarse grid for almost the entire fluid domain, except in a narrow band around the fluid-solid boundary, where it is solved at a finer resolution. The coarser solution is then upgraded to a finer grid everywhere in the fluid domain, while correctly enforcing all boundary conditions. In the next section we explain the basic ideas behind the narrow band pressure solve and the upgradation strategies.

### 4 NARROW BAND PRESSURE SOLVE

There are two regions in the fluid where resolving the fluid accurately is essential. The first of these is the fluid-solid boundary. In order to resolve the details at such boundaries, we create a narrow band of fine grid cells around all solid boundaries. Examples of this are shown in Figure 1.

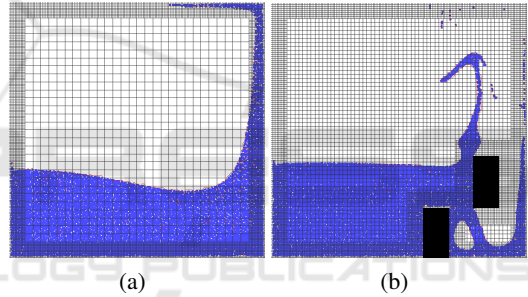


Figure 1: The narrow band of fine grid cells can be seen around all solid boundaries. 1(a) shows the coarse grid with 1 coarse grid cell equal to 16 fine grid cells and narrow band of fine cells that is 8 fine grid cells wide. 1(b) shows the coarse grid with 1 coarse grid cell equal to 4 fine grid cells and narrow band of fine cells that is 8 fine grid cells wide. Here the narrow band can be seen around the solid obstacles as well.

Post velocity advection, the Poisson equation is solved on the coarse and narrow band fine grid using a preconditioned conjugate gradients solver. Any other solver of choice can also be used for this step. If these two grids are used directly to advect the fluid surface, the coarse grid is not able to resolve the fluid surface accurately due to its Nyquist limit. This is the second region where the fluid needs to be accurately resolved, else all visual details are lost. In order to do this, the coarse grid has to be upgraded to a finer grid everywhere in the fluid domain, post the narrow band pressure solve.

The fundamental idea behind the need for upgradation here is to get velocity on a finer grid everywhere before the fluid surface is advected. This al-

lows the velocity field to have enough degrees of freedom to accurately resolve free surface detail. This velocity field also has to be divergence free to enforce mass conservation in the fluid.

We tried two methods for performing the upgradation. We call these methods upgradation by velocity interpolation and by pressure field smoothing. We describe both below.

## 4.1 Upgradation by Velocity Interpolation

The first method upgrades the velocity field in the coarse grid, after the pressure solve. We create a new fine grid everywhere in the fluid domain. At the boundary between the coarse and the narrow band fine grid, velocity is interpolated between the narrow band values and the coarse grid values from the neighbouring cells and the interpolated value is copied to the new fine grid. Everywhere else, the value from the underlying grid (coarse or narrow band fine) is copied as is. Now, the final velocity field is available in a fine grid everywhere in the fluid domain before the liquid surface is advected and there are enough degrees of freedom present to compute adequate surface detail. Algorithm 1 explains what happens in one simulation step when using this method.

---

Algorithm 1: Single time step algorithm with velocity field interpolation.

---

- 1: Advect  $\mathbf{u}^n$  to  $\mathbf{u}^*$  using Equation 3 on the fine grid everywhere in the fluid domain.
  - 2: Solve Poisson system given by Equation 4 on the coarse grid.
  - 3: Solve Poisson system given by Equation 4 on the narrow band fine grid.
  - 4: Compute velocity  $\mathbf{u}^{n+1}$  on the coarse and narrow band fine grids using Equation 5.
  - 5: Interpolate the velocity field across the coarse and narrow band fine grid boundary.
  - 6: Copy interpolated velocity to the new fine grid.
  - 7: Extrapolate velocity from the fine grid.
  - 8: Compute the distance field  $\phi$  using Equation 6 and advect the liquid surface.
- 

This method is easy to compute as the interpolation adds minimal overhead to the computation cost. We, however, found that when the narrow band is smaller in width than a fourth of the original (i.e., non-coarse) grid size, the fluid loses mass rapidly, as errors in the velocity field dominate. The maximum speedup obtained is thus limited when using this upgradation method. It is also harder to ensure that the final upgraded velocity field on the fine grid is divergence

free. Therefore, the method suffers from mass loss errors.

## 4.2 Upgradation by Pressure Field Smoothing

In our next method instead of upgrading the velocity field, we upgrade the pressure field itself. In order to do this, the pressure field is interpolated across the coarse and narrow band fine grid boundary. Then the pressure field is regularized by running 1 – 3 Jacobi iterations on it. We start by initializing the iteration using the interpolated pressure field on the fine grid and then solve Equation 4 using the Jacobi iterations. This ensures that the interpolated field is free from divergence, as is the subsequent velocity field computed from it. This is then used to advect the liquid surface. This method does not suffer from significant mass loss like the velocity interpolation method, and with careful implementation the Jacobi iteration does not pose too much of an additional computational burden. Algorithm 2 presents the steps involved in this method.

The pressure smoothing technique allows us to get large speedups over a conjugate gradient solve everywhere on a fine grid, without sacrificing the fluid surface details. This makes it very suitable for visual fluid simulation.

---

Algorithm 2: Single time step algorithm with pressure field smoothing.

---

- 1: Advect  $\mathbf{u}^n$  to  $\mathbf{u}^*$  using Equation 3 on the fine grid everywhere in the fluid domain.
  - 2: Solve Poisson system given by Equation 4 on the coarse grid.
  - 3: Solve Poisson system given by Equation 4 on the narrow band fine grid.
  - 4: Interpolate the pressure field across the coarse and narrow band fine grid boundary.
  - 5: Copy interpolated pressure to the new fine grid.
  - 6: Run upto 3 Jacobi iterations on the pressure field in the fine grid to regularize it.
  - 7: Compute velocity  $\mathbf{u}^{n+1}$  on the fine grid using the regularized pressure field using Equation 5.
  - 8: Extrapolate velocity from the fine grid.
  - 9: Compute the distance field  $\phi$  using Equation 6 and advect the liquid surface.
- 

## 4.3 Boundary Conditions

There are usually two kinds of boundaries in a free surface fluid simulation. The boundary between the fluid and the solid requires a Neumann boundary condition, which is enforced for all cells in the nar-

row band when the narrow band Poisson equation is solved. The free surface requires a Dirichlet boundary condition, which is carefully enforced for all cells on the fluid surface during the Poisson solves and the interpolation done for the pressure field smoothing. A third boundary is introduced in the simulation due to partitioning the fluid domain in coarse and narrow band fine cells. Fluid is allowed to move freely across this boundary so that this boundary appears completely porous to the fluid during advection.

## 5 EXPERIMENTAL RESULTS AND ANALYSIS

We have performed a number of experiments to catalog the efficacy of our methods and also to determine the kind of errors introduced in the simulation due to its use. We have performed all our experiments on a machine with a 16 core Intel 2.60 GHz Xeon processor with 32 GB of RAM. We solve the Navier-Stokes by splitting the equations, using operator splitting, into advection and pressure projections stages. The pressure projection step needs to solve a large linear system at each time step of the simulation. An incomplete Cholesky preconditioned conjugate gradient technique is used to solve the voxelized Poisson equation in this stage (Bridson, 2008). We use this solver as a base solver in all our simulations. Our base fluid simulator is parallelized using OpenMP, with the exception of the preconditioned conjugate gradient pressure solver, which is implemented serially. This same solver is used for the Poisson solves in our narrow band simulator as well.

### 5.1 Performance with Velocity Interpolation

We applied velocity interpolation based upgradation (see Section 4.1) to grids with fine narrow bands of width 64 and 128 cells. Average iteration time, averaged over every 500 frame window, is plotted and shown in Figure 2 for the narrow band width of 64. It should be noted that narrow band widths are always measured in number of fine grid cells. The original base simulation is a simple dam-break simulation, run on a  $512 \times 512$  fine grid. In the coarse grid, the coarse grid cell size used is double the size of the fine grid cell size in either dimension. The speedup obtained in total simulation time is 22.9% and 20.0% for the 64 and 128 sized narrow bands respectively. Reducing the narrow band grid size below 64 pushes errors in velocity beyond acceptable limits.

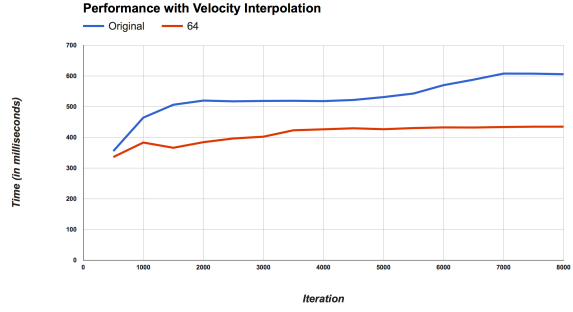


Figure 2: Performance of the fluid simulation when using the velocity interpolation method with a narrow band of width 64.

### 5.2 Performance with Pressure Field Smoothing

Next, we applied pressure field smoothing upgradation (see Section 4.2) to grids with fine narrow bands of widths ranging from 8 to 64. The pressure field smoothing method allows much thinner narrow bands of fine grid cells with less error, thereby offering much larger speedups. The original base simulation is the same as the one used above. Average iteration time, averaged over every 500 frame window, is plotted and shown in Figure 3. In each case, 3 Jacobi iterations were run to regularize the interpolated pressure field.

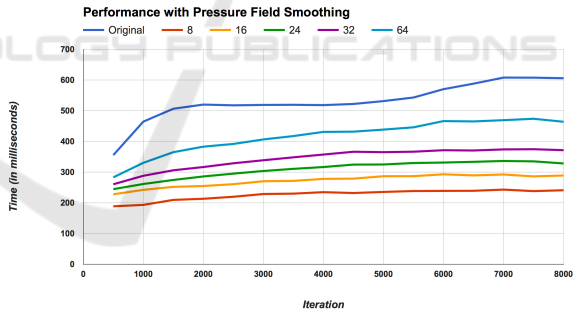


Figure 3: Performance of the fluid simulation when using the pressure field smoothing method. Here 1 coarse grid cell is equal to 4 fine grid cells.

We further pushed the amount of speedup that can be obtained with our technique by making the coarse grid cells larger to contain 16 fine grid cells instead of the earlier 4. The average iteration time is plotted as before in Figure 4. The speedup obtained in total simulation time in each case is shown in Table 1. The second column of the table gives the speedup when 1 coarse grid cell contains 4 fine grid cells, and the third column when 1 coarse grid cell contains 16 fine grid cells.

Figure 5 shows a comparison of the per iteration performance of the original simulator with the

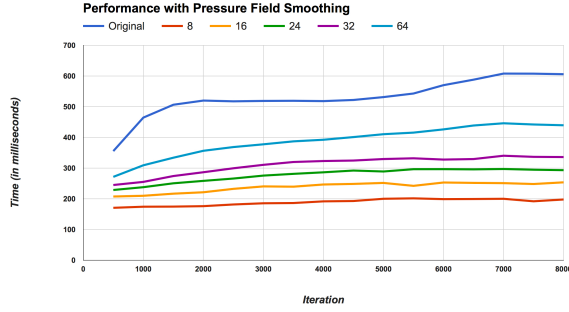


Figure 4: Performance of the fluid simulation when using the pressure field smoothing method with larger coarse grid cells. Here 1 coarse grid cell is equal to 16 fine grid cells.

Table 1: Percent speedup obtained in total simulation time over the original base simulation for different narrow band widths.

| Width of narrow band | Speedup (Coarse 4) | Speedup (Coarse 16) |
|----------------------|--------------------|---------------------|
| 8                    | 57.5%              | 64.4%               |
| 16                   | 48.9%              | 55.1%               |
| 24                   | 42.1%              | 47.7%               |
| 32                   | 35.5%              | 41.5%               |
| 64                   | 21.9%              | 26.8%               |

fastest velocity smoothing case and the fastest pressure smoothing case, for the first 100 iterations of the simulation. This is comparison of raw per iteration timing data, without the averaging done in the previous cases. It can be clearly seen that the pressure field smoothening method gives very large speedups in comparison to the velocity interpolation method, for the same original base simulation. We will see later that it also produces less error in the simulation. We compare the visual quality of the simulations produced next.

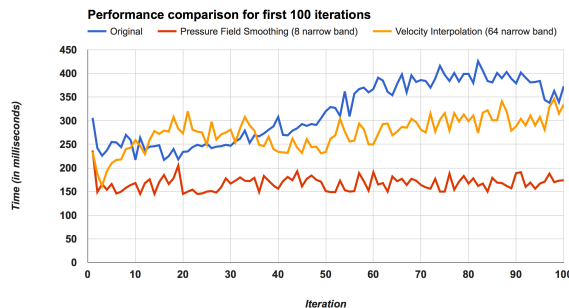


Figure 5: Comparison of performance of various implementations of the fluid simulator for first 100 iterations.

### 5.3 Visual Quality Comparison

Figure 6 shows rendered frames from the original 2D simulator, and the same frames from the simulators implemented with velocity interpolation and pressure

field smoothing at different coarse grid resolutions. It can be seen that the pressure field smoothing results are visually closer to the original, unaccelerated simulator. The velocity interpolation method introduces artefacts in the simulation in the form of additional air gaps in the fluid volume and also, mass loss. The size of the narrow band is 64 with velocity interpolation and 8 with pressure field smoothing. Between the two pressure smoothing cases some difference can be seen, owing to the difference in size of the coarse grid cells.

We also show some more frames from another simulation that had additional solid obstacles in the fluid domain in Figure 7. The narrow band also exists around the obstacles. It can be seen that our method correctly resolves all simulation details even around the obstacles.

Comparison videos of these simulations can be seen in the supplementary video submitted with the paper.

### 5.4 3D Simulation

We performed similar experiments on a 3D fluid simulator. The methods introduced in this paper work perfectly in 3D too. The speedup in total simulation time obtained with pressure field smoothing over an original base dam break simulation on a grid size of  $128 \times 128 \times 128$  is 38.0%. This is with a narrow band size of 24 and with 1 coarse grid cell equal to 8 fine grid cells. Sample rendered frames of the simulation can be seen in Figure 8. Visual quality of the results generated by the pressure field smoothed simulator is comparable to the original unaccelerated simulator.

### 5.5 Error Analysis

We compute the error introduced in the simulation due to the approximation introduced by the coarse grid. We show the difference in velocity in the horizontal and vertical directions in the fluid field in Figure 9, for a single frame. Warmer colors represent higher error. It can be seen that the velocity interpolation method introduces more error in the fluid than the pressure smoothing case. Errors also increase as the coarse grid cell size increases and narrow band width decreases (see Figure 10). Visual fidelity of the simulation and error have to be balanced against the speedup obtained during simulation based on computational requirements and costs.

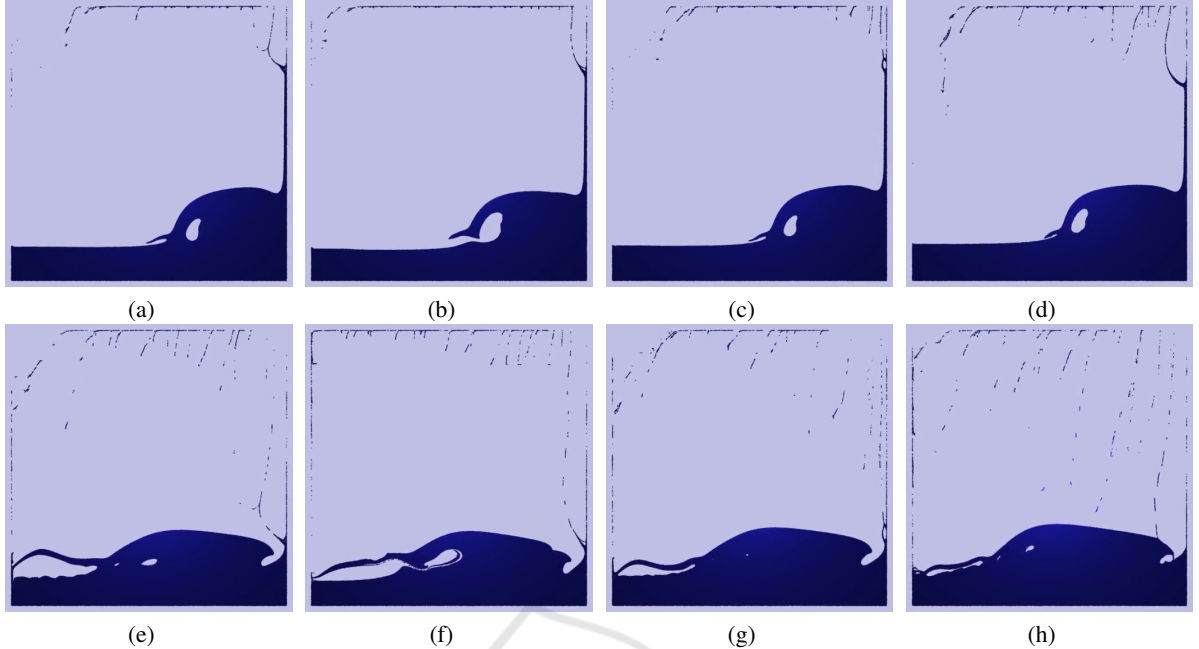


Figure 6: Comparison of visual quality of the simulation produced. 6(a) and 6(e) are two different frames from the original simulation, 6(b) and 6(f) are the same frames from the simulator implemented with velocity interpolation, 6(c) and 6(g) are frames from the simulator implemented with pressure field smoothing on coarse grid cell size equal to 4, 6(d) and 6(h) are frames with pressure field smoothing on coarse grid cell size equal to 16 fine grid cells.

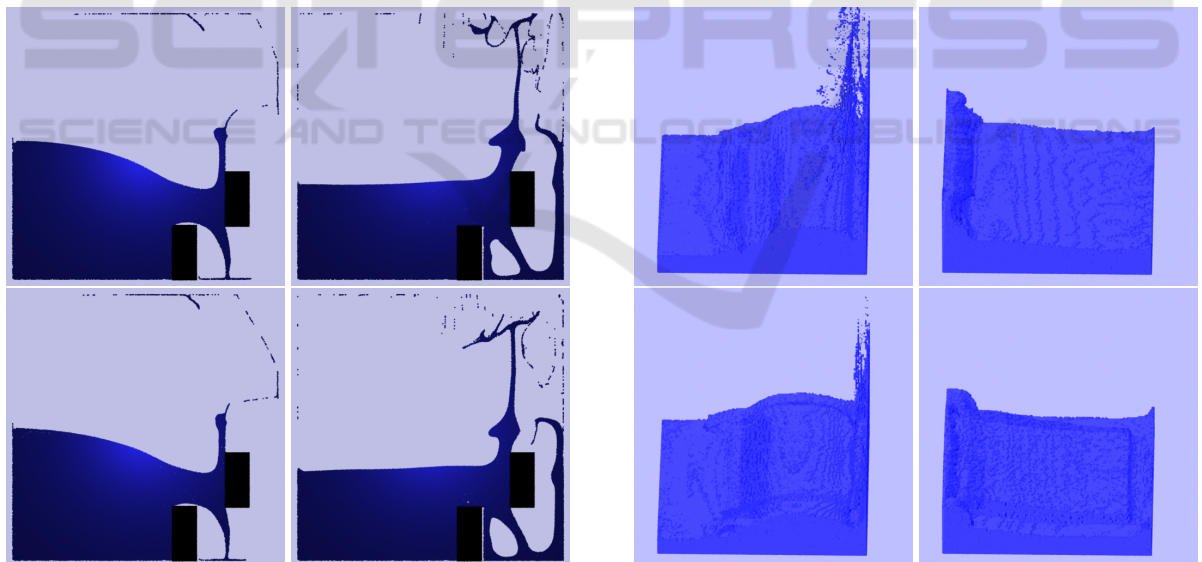


Figure 7: Comparison of visual quality of the simulation produced with obstacles in the fluid. The top row shows frames from the original simulation on a  $256 \times 256$  grid. The bottom row shows the same frames from the simulator with pressure field smoothing, with 1 coarse grid cell size equal to 4 fine grid cells and a narrow band of width 8.

Figure 8: Comparison of visual quality of the simulation produced in 3D. The top row shows frames from the original simulation on a  $128 \times 128 \times 128$  grid. The bottom row shows the same frames from the simulator with pressure field smoothing on a coarse grid with a narrow band of width 24.

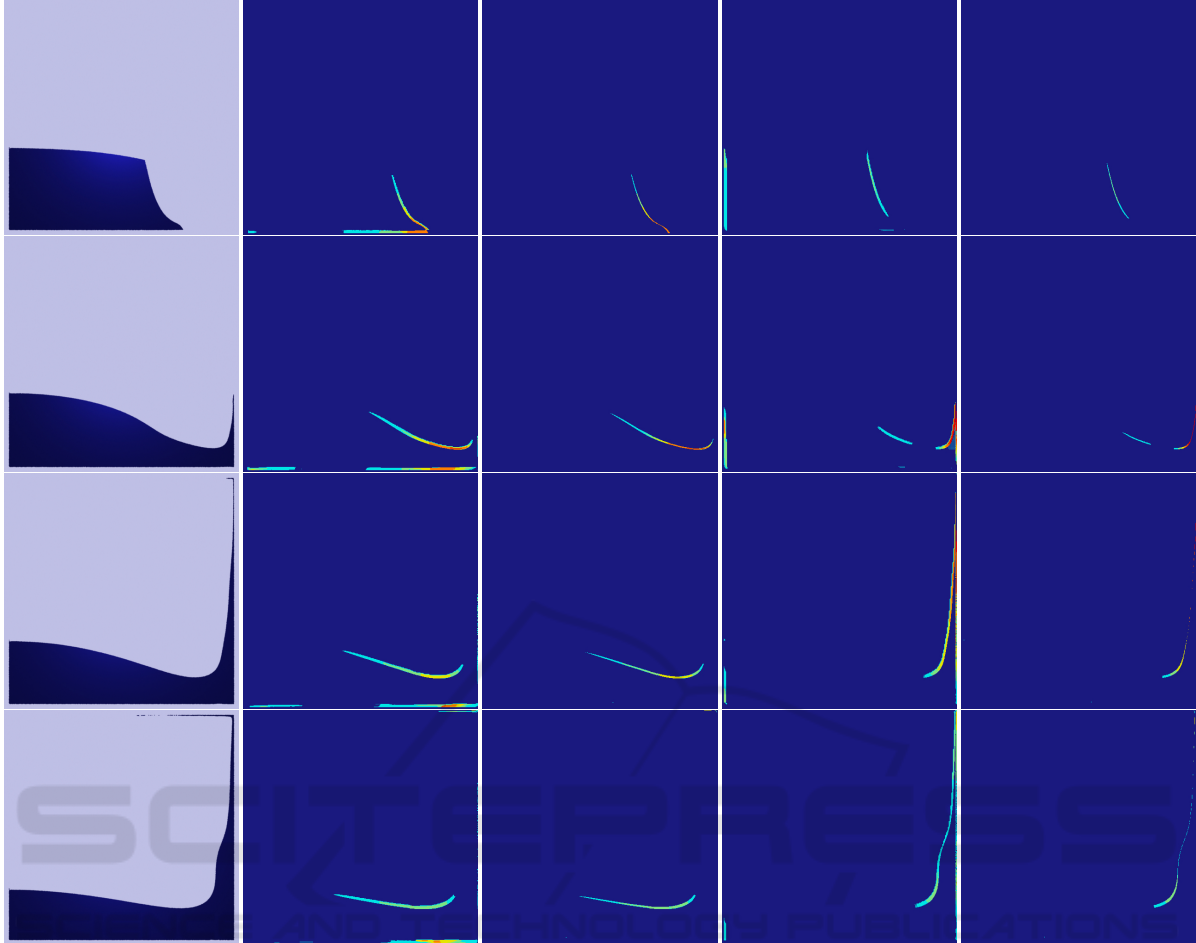


Figure 9: Comparison of error in fluid velocity. The first column shows frames 1000, 2000, 3000 and 4000 from the original simulation, the second and third columns show error in the horizontal component of velocity for velocity interpolation and pressure smoothing, the fourth and fifth columns show error in vertical component of velocity for velocity interpolation and pressure smoothing respectively. Blue represents 0 error and red represents maximum error.

## 6 CONCLUSIONS

We have presented a method to accelerate the pressure projection step in an Eulerian fluid simulator by solving the Poisson's equation only in a narrow band around fluid-solid boundaries. We solve this system of equations on a coarser grid everywhere else in the fluid domain and then upgrade this result to a finer grid to obtain enough degrees of freedom to track the fluid surface accurately. We present two methods of performing the upgradation, namely velocity interpolation and pressure field smoothing. We compare the pros and cons of each, giving extensive results about the visual quality of simulations produced, errors introduced in the simulation and the computation speedup obtained. We conclude that the pressure field smoothing method performs better on all metrics and

is a better way to perform the upgradation than velocity interpolation. We also show that the same methods work in a 3D fluid simulator also.

The behaviour of the narrow band computation in the presence of more complicated, non-grid aligned obstacles needs more analysis. The role of the size of the obstacle with respect to the grid size also needs to be carefully understood. Currently, we have used a small and conservative timestep size in the narrow band simulator. We would like to investigate adaptive timestepping for such simulators as well.

We would like to explore adaptive grid coarsening during every step of the simulation so that adequate degrees of freedom are always available at the fluid surface to resolve detail. This will help us avoid the grid upgradation step and may lead to better performance. We also want to explore the use of our method

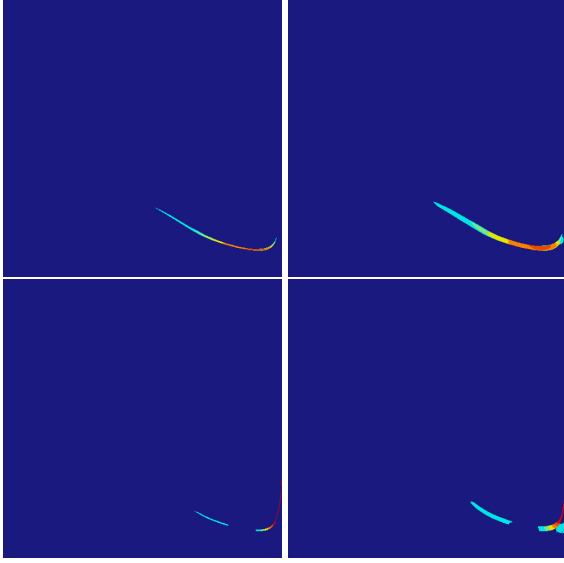


Figure 10: Comparison of error in fluid velocity between different coarse grid resolutions when using pressure smoothing. The first column shows error in horizontal and vertical components of velocity when 1 coarse grid cell contains 4 fine grid cells, the second column shows the same errors when 1 coarse grid cell contains 16 fine grid cells. The error regions are wider for coarser grids.

in accelerating other fluids simulations such as smoke and fire.

## REFERENCES

- Ando, R., Thuerey, N., and Wojtan, C. (2015). A dimension-reduced pressure solver for liquid simulations. *Computer Graphics Forum*, 34(2):473–480.
- Autodesk. Deep adaptive fluid simulation in Maya 2016. <http://www.autodesk.com/products/maya/features/dynamics-and-effects/deep-adaptive-fluid-simulation>. Last accessed on 8/6/2016.
- Berger, M. and Oliger, J. (1984). Adaptive mesh refinement for hyperbolic partial differential equations. *Journal of Computational Physics*, 53:484–512.
- Bridson, R. (2008). *Fluid Simulation for Computer Graphics*. Taylor & Francis.
- Bridson, R., Hourihane, J., and Nordenstam, M. (2007). Curl-noise for procedural fluid flow. *ACM Transactions on Graphics*, 26(3).
- Chentanez, N. and Müller, M. (2011). Real-time eulerian water simulation using a restricted tall cell grid. In *ACM Transactions on Graphics*, volume 30, page 82.
- Chentanez, N., Müller, M., and Kim, T.-Y. (2014). Coupling 3d eulerian, heightfield and particle methods for interactive simulation of large scale liquid phenomena. In *Proceedings of the ACM SIGGRAPH/Eurographics SCA*, pages 1–10.
- De Witt, T., Lessig, C., and Fiume, E. (2012). Fluid simulation using laplacian eigenfunctions. *ACM Transactions on Graphics*, 31(1):10:1–10:11.
- Enright, D., Marschner, S., and Fedkiw, R. (2002). Animation and rendering of complex water surfaces. *ACM Transactions on Graphics*, 21(3):736–744.
- Ferstl, F., Ando, R., Wojtan, C., Westermann, R., and Thuerey, N. (2016). Narrow band FLIP for liquid simulations. *Computer Graphics Forum (Eurographics)*, 35(2):to appear.
- Ferstl, F., Westermann, R., and Dick, C. (2014). Large-scale liquid simulation on adaptive hexahedral grids. *IEEE Transactions on Visualization and Computer Graphics*, 20(10):1407–1417.
- Foster, N. and Fedkiw, R. (2001). Practical animation of liquids. In *Proceedings of SIGGRAPH*, pages 23–30.
- Jung, H. R., Kim, S.-T., Noh, J., and Hong, J.-M. (2013). A heterogeneous CPUGPU parallel approach to a multigrid poisson solver for incompressible fluid simulation. *Computer Animation and Virtual Worlds*, 24(3–4):185–193.
- Kim, T., Tessendorf, J., and Threy, N. (2013). Closest point turbulence for liquid surfaces. *ACM Transactions on Graphics*, 32(2):15:1–15:13.
- Larmorlette, L. and Foster, N. (2002). Structural modeling of flames for a production environment. *ACM Transactions on Graphics*, 21(3):729–735.
- Lentine, M., Zheng, W., and Fedkiw, R. (2010). A novel algorithm for incompressible flow using only a coarse grid projection. *ACM Transactions on Graphics*, 29(4).
- Losasso, F., Gibou, F., and Fedkiw, R. (2004). Simulating water and smoke with an octree data structure. *ACM Transactions on Graphics*, 23(3):457–462.
- McAdams, A., Sifakis, E., and Teran, J. (2010). A parallel multigrid poisson solver for fluids simulation on large grids. In *Proceedings of ACM SIGGRAPH/Eurographics SC*, pages 65–74.
- Montijn, C., Hundsorfer, W., and Ebert, U. (2006). An adaptive grid refinement strategy for the simulation of negative streamers. *Journal of Computational Physics*, 219(2).
- Mullen, P., Crane, K., Pavlov, D., Y., T., and Desbrun, M. (2009). Energy-preserving integrators for fluid animation. In *Proceedings of SIGGRAPH*, pages 1–8.
- Prakash, A. and Chaudhuri, P. (2015). Comparing performance of parallelizing frameworks for grid-based fluid simulation on the cpu. In *Proceedings of the 8th ACM India Computing Conference, Compute ’15*, pages 1–7.
- Rasmussen, N., Nguyen, D., Geiger, W., and Fedkiw, R. (2003). Smoke simulation for large scale phenomena. *ACM Transactions on Graphics*, 22(3):703–707.
- Schechter, H. and Bridson, R. (2008). Evolving sub-grid turbulence for smoke animation. In *Proceedings of the ACM SIGGRAPH/Eurographics SCA*, page 17.
- Selle, A., Fedkiw, R., Kim, B., Liu, Y., and Rossignac, J. (2008). An unconditionally stable maccormack method. *Journal of Scientific Computing*, 35(2–3):350–371.
- Stam, J. (1999). Stable fluids. In *Proceedings of SIGGRAPH*, pages 121–128.

- Stomakhin, A., Schroeder, C., Chai, L., Teran, J., and Selle, A. (2013). A material point method for snow simulation. *ACM Transactions on Graphics*, 32(4):102:1–102:10.
- Threy, N., Wojtan, C., Gross, M., and Turk, G. (2010). A multiscale approach to mesh-based surface tension flows. *ACM Transactions on Graphics*, 29(4).
- Treuille, A., Lewis, A., and Popovi, Z. (2006). Model reduction for real-time fluids. *ACM Transactions on Graphics*, 25(3):826–834.
- Yue, Y., Smith, B., Batty, C., Zheng, C., and Grinspun, E. (2015). Continuum foam: A material point method for shear-dependent flows. *ACM Transactions on Graphics*, 34(5):160:1–160:20.

